

Tritium depth profiles and accelerator mass spectroscopy for JET tiles (graphite/CFC tiles)

N.Bekris¹, M. Glugla¹, U. Berndt¹, R.-D.Penzhorn¹, M. Friedrich² W. Pilz²,

¹Forschungszentrum Karlsruhe, Tritium Labor (TLK) P.O.Box 3640, 76021 Karlsruhe, Germany

²Forschungszentrum Rossendorf, P.O.Box 510119, 01314 Dresden, Germany

1. Introduction

Tritium retention in carbon first wall tiles is an important issue not only from a radiological point of view but also for inventory purposes. As the divertor vertical targets of the ITER machine are constituted from carbon tiles, it is of paramount importance to evaluate the amount of tritium that may be retained by these tiles. For that purpose a total of 24 tiles were removed from the divertor (10), the inner guard limiter (6) and the poloidal limiter (8) from the JET fusion machine after the first Deuterium-Tritium Experiment (DTE1) and sent to the Tritium Laboratory in Karlsruhe (TLK) for a surface and bulk tritium analysis.

Due to plasma wall interactions a fraction of the fuelled tritium becomes incorporated into the first wall materials of fusion machines, so it is expected that they will be tritium-contaminated.

In addition, during plasma discharges hydrogen isotopes are implanted into the graphite tiles as ions or as energetic neutral atoms having lost their charges after one or several electron captures (charge-exchange mechanism). Complex processes, different to some extent from those known in metals, govern the transport of hydrogen in graphite [1]. Plasma particles interact not only with the outer surfaces of the first wall but also after diffusion with the inner surfaces of the interconnected pores. Hydrogen atoms may also combine with the eroded carbon to form a hydrocarbon film which is co-deposited on the surface of the tiles. In other areas of the tiles the implanted hydrogen combines with the

carbon to form a hydrogenated carbon layer whose thickness depends on the energy of the more energetic particles. Retention via co-deposition and implantation of energetic ions into the near surface layers as well as bulk effects including migration through the network of interconnected pores and diffusion across the grains are dependent on the plasma operation conditions (electron temperature, electron density) and on the degree of neutron and alpha irradiation damage [2]. It is known that hydrogen implanted at room temperature is retained at the near surface until a saturation is reached [3, 4]. The saturation concentration has been reported to be in the H/C ratio range of 0.3 - 0.6 [5] and depends on the prevailing temperature. The films found in the relatively cool (< 200°C), shadowed area (not subjected to plasma bombardment) are very rich in hydrogen content. The H/C ratio measured by Ion Beam Analysis (IBA), showed a value between 0.7 – 0.8 [6] It depends also on the implantation energy (incident ion energy at JET < 50 eV) but seems to be relatively insensitive to the microstructure of the carbon [7].

2. Experimental

2.1. Full combustion

The tritium determination was achieved using the full combustion technique proposed by Vance et al. [8]. The glass experimental arrangement used at the TLK is shown schematically in figure 1. A stream of pure air from a pressurised cylinder was used with a flow

rate of approx. 15 cm³/min. Passing the air through a bubbler containing water ensured the carrier gas was humidified.

Cylinders retrieved from selected zones of the various tiles having a diameter of 7.8 mm were sliced into small disks having a thickness of 1 mm employing a diamond-grinding disk. The grinding disk was rotated with only 100 rpm to avoid unnecessary heating of the cylinder. To minimise cross-contamination the diamond-grinding disk was cleaned after each cutting.

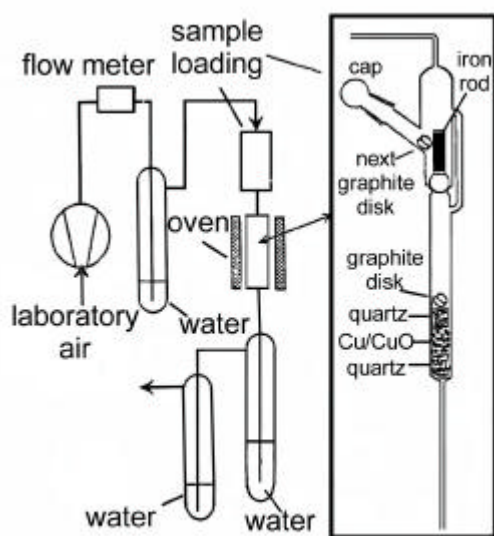


Fig.1. Schematic view of the combustion apparatus used at the TLK.

Graphite or CFC disks were introduced via a joint into a small receptacle placed on top of the combustion zone and isolated from this zone by a glass-to-glass seal. To introduce the graphite disk into the combustion zone the seal was lifted from the outside with two appropriate magnets. The combustion zone itself consists of a vertically arranged quartz tube heated from the outside with a cylindrical oven designed for temperatures of up to 1500 °C. The actual sample temperatures were determined with a thermocouple placed inside of the quartz tube. The combustion tube itself contained approx. 30 g of a wire packing consisting of a Cu₂O core with CuO on the surface.

The packing is secured between two pieces of quartz wool packing, on top of which the disk to be analysed drops by gravity when the seal is opened. The copper oxide contributes to ensure complete oxidation of all molecular hydrogen isotopes and all hydrocarbons released during the combustion of the disks. The effluent gases are then passed through a bubbler containing water (about 200 cm³) via the shortest route. By this procedure the quartz tube, extending from the combustion zone down to the water level in the bubbler, remains at all times at comparatively high temperature. The experimental evidence indicates that most of the tritiated water (> 99%) is retained in this first bubbler. To assure quantitative trapping of the tritiated water, a second bubbler, also filled with water is placed downstream.

After each combustion 50 µl water aliquots were taken from the first bubbler and 1 ml from the second employing calibrated syringes. These aliquots were mixed with 15 cm³ of a scintillation cocktail and analysed for total tritium with a liquid scintillation counter (LSC). The LSC instrument employed at the TLK is a Tri-Carb 2300TR Liquid Scintillation Analyser from Packard. Upon completion of an analysis the surface contamination remaining on the tubing inserted into the water of the first bubbler was removed by rinsing thoroughly several times with fresh water. Frequent blank tests without sample or with virgin graphite disks were carried out to verify that no cross contamination had taken place.

2.2. AMS

In order to have more accurate concentration profiles in the micro-meter range the accelerator mass spectrometry (AMS) was used. The method is a combination of secondary negative ion mass spectrometry coupled to nuclear physics instruments and devices as are the tandem accelerator or the isotope separation and detection instruments [9].

The principle of tandem accelerator mass spectrometry is described below and a schematic view of the experimental set-up used at the Forschungszentrum Rossendorf is shown in Fig. 2.

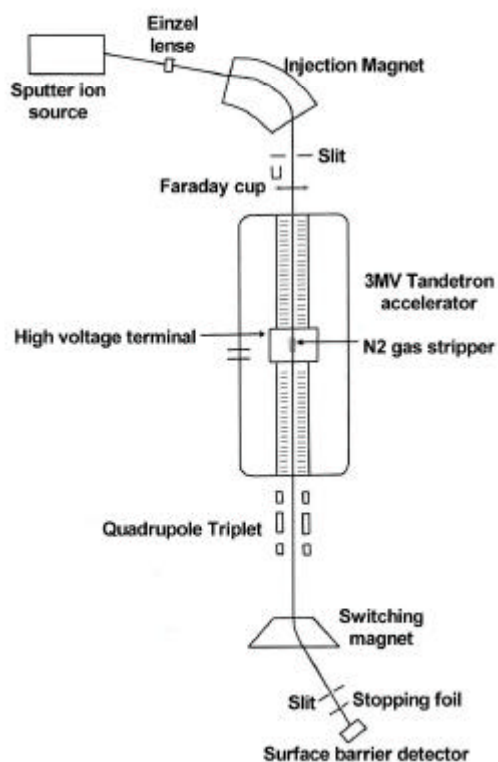


Fig. 2. Schematic illustration of the AMS experimental set-up in Rossendorf.

The following is a brief description of each element of the AMS system.

The sputter ion source produces a beam of caesium ions. The caesium gas flows into the ion source after the caesium reservoir is heated. After being surface ionised with a hot spherical tungsten ionizer the Cs^+ beam is focused on the investigated sample, which is set on a negative voltage of -3 kV giving a cathode current of about 1 mA. Using a mechanical wobbling mechanism the sample crater was changed from a bell-like shape to cylindrical shape with a surface area of a parallelogram of about $2.5 \times 2.5 \text{ mm}^2$. The Cs^+ beam spot has a FWHM of about $400 \mu\text{m}$. Due to the uniform erosion inside the cylindrical sputter crater the concentration depth profile is converted

into a time dependent particle beam from the ion source.

The injection magnet is double focusing and provides mass analysis of the secondary negative ions after being extracted from the ion source by a voltage of 23 kV. The injection magnet bends the negative ion beam by 80° to select certain mass atoms or molecules. Some pumps provide a vacuum of about 10^{-6} mbar inside the beam-line. Before the negative ions reach the accelerator a retractable Faraday cup was sometimes used for the measurement of the high intensity components such as deuterons and carbon.

The tandem accelerator consists of two accelerating gaps with a large positive voltage in the middle. Part of it is a large pressure vessel containing the SF_6 insulating gas at a pressure of 8 bar. The negative ions travelling down the beam tube are accelerated towards the positive terminal. At the terminal they are passed through a nitrogen gas electron stripper and emerge as positive ions. These are repelled from the positive terminal, accelerating again to ground potential at the exit of the accelerator. The name tandem accelerator comes from this dual acceleration concept. The Rossendorf Tandetron can be operated at a maximum voltage of 3 MV but for tritium the optimised terminal voltage was found to be about 1.5 MV.

The analysing and switching magnet are employed for further mass separation. The negative ions with mass 3 (T^- , HD^- , H_3^-) selected by the injection magnet are accelerated by the Tandetron. The T^+ ions generated by stripping are further accelerated by the high energy acceleration tube and acquire an energy of up to 3 MeV, while the HD^+ or the atomic H_3^+ ions generated by charge exchanges in the stripper disintegrate immediately into atomic ions. The more stable charged atomic ions (H^+ and D^+) having lower energies and masses than tritium are easily suppressed by the 30° switching magnet having a radius of curvature of about

1.4 m. Only a very small fraction of the negative molecular ions undergoes a charge-exchange and turn into positive molecular ions (HD^+) which could be counted as tritium.

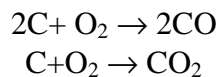
The surface barrier detector is used to count the ions. The molecular ions passing the switching magnet together with the 3 MeV tritium ions are finally stopped by a 17 μm thick Al foil installed in front of the implanted silicon detector. The few HD^+ ions in the beam were cracked in the stopping foil to 1 MeV protons and 2 MeV deuterons, while H_3^+ ions are converted to 1 MeV protons. The 1 MeV protons are stopped inside the foil, while the deuterons passes the foil with lower energy than the tritium ions and can be separated in the energy spectrum of the detector.

2.2.1. AMS on high tritium samples

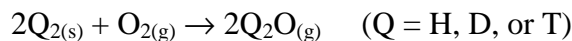
In order to prevent any contamination of the versatile Tandetron during measurements of samples with high tritium inventory a dedicated AMS facility with a 100 kV tandem accelerator was constructed and put into operation at the Forschungszentrum Rossendorf [10]. Instead of a gas stripper this tandem accelerator is equipped with a long-lived carbon foil for electron stripping.

3. Results and discussion

The full combustion technique implies carbon oxidation. The involved reactions are:

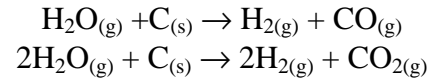


In the same way all hydrogen isotopes trapped, bonded or even co-deposited in the carbon surface will also be oxidised according to the reaction



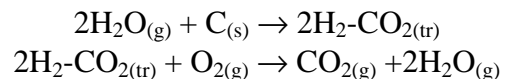
and condensed as liquid into the bubbler located downstream.

There are experimental indications that the presence of moisture is necessary for the full combustion of charcoal [11]. For the quantitative determination of tritium in a solid by full oxidation a moist carrier gas is also recommended to minimise memory effects [12, 13]. Therefore, it is necessary to consider the reactions of carbon with steam. The overall reaction can be described by:



In this oxidation path the oxygen is supplied by the water which decomposes to carbon dioxide (or monoxide) and hydrogen. Nevertheless, water is almost always observed as a reaction product instead of molecular hydrogen.

The most probable mechanism involves the interaction of water with carbon. In a first step, water is adsorbed on the carbon surface [14]. This adsorption starts at relatively low temperatures (400 °C) generating a transient species. This step is followed by the evolution of the transient species to give carbon dioxide and water. The whole process is described below:



In the following section, the combustion results obtained with samples from a TFTR and a JET tile are discussed in detail.

3.1. Tritium profile of JET CFC tile IN3_{s1}

The analysis of deuterium retained in the JET fusion machine revealed a non-uniform distribution of the retention over the vessel [15, 16]. During DTE1 the torus retained about 40% of the introduced tritium [17]. Numerous tritium analyses have also revealed that the most of the tritium retained by the vessel is located in the inner divertor region especially in tiles 3 and 4 [18]. A cross section of the JET

Mark IIA divertor including the tritium surface concentration measured by the full combustion technique in MBq/cm² is shown in figure 3.

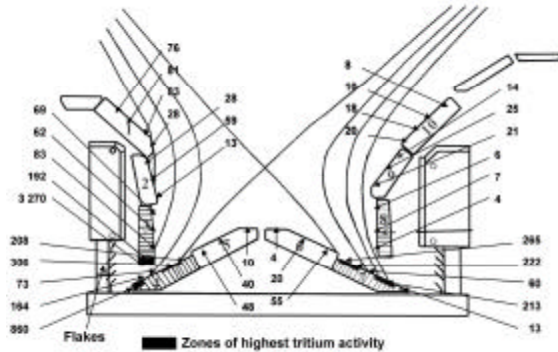


Fig. 3. Cross section of the MKIIA divertor in JET. The illustrated surface tritium activities are in MBq/cm².

Starting from the inner divertor region (top tile 1) and going along the poloidal direction (next divertor tiles) the tritium surface concentration increases gradually showing a peak maximum for the edge of the tile 3 and the bottom of the tile 4 (3270 MBq/cm² and 860 MBq/cm² respectively). These positions are actually in zones not accessible to the plasma (shaded zones). It appeared that these parts of the tiles are coated with a thick film of co-deposited material (flakes, dust,) which in some parts is so thick that it has flaked off and dropped down into the bottom of the vessel.

From the bottom of tile 4 and across the rest of tile 5 the surface tritium concentration shows a notable decrease and reaches its minimum on the top of the divertor dome (10 MBq/cm²). A similar pattern is observed starting from the top of tile 6 and going across the outer divertor. However, surprisingly there is no co-deposit or flakes on the edge of tile 8 as it was found for the symmetric tile number 3. The peak maximum is located once again in the strike region of tile 7. The same pattern was observed in deuterium analyses of the same tiles [19].

Besides these surface tritium concentrations, the tritium activity in the

bulk of the tiles, particularly for tiles 3, 4 and 7, was also measured and the results concerning tile 3 will be presented hereafter.

Using a hollow drill several cylinders were retrieved from the plasma exposed surface of tile 3 as well as from its shadowed edge [figure 1 ref.20]

The cylinders were cut to small disks using the technique described above and combusted individually in the Vance's apparatus. Tritium was analysed by liquid scintillation.

As it is illustrated in figure 4 there is clearly a diffusion profile through the whole tile as it was already found out by PIN diode measurements [20]. We must also notice that the x scale in the figures is in millimetres and the last point in each figure represents the back side of the tile.

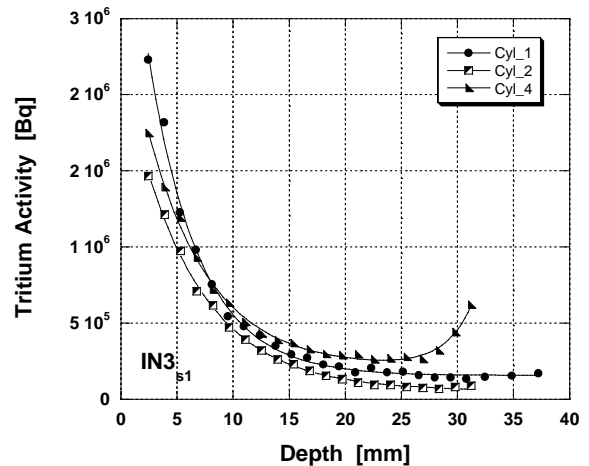


Fig 4. Tritium profiles for IN3_{s1} determined by full combustion of small disks having 1 mm thickness and 7.6 mm diameter.

The diffusion profile is clearly exponential and it was possible to fit it with an equation of the type

$$A = A_B + A_0 \cdot e^{(-kD)},$$

where A is the tritium activity measured or calculated (for the part lost during cuts), A_B the activity in the bulk of the tile D the depth and k is a constant having an inverse length dimension and being dependent on

the temperature and the nature of the tile (graphite or CFC). For the CFC tile number 3 the k value is fairly constant and about 0.2 mm^{-1} . A_0 represents the tritium activity on the surface of the tile (this does not include the tritium content of any deposited film on top of the surface).

The surface activity of each cylinder is not illustrated in the figure 4. Indeed, a lot of co-deposited material coats the plasma exposed surface of that tile, so that the first disk contains a significant amount of tritium and therefore it is omitted from the figures as it is always off-scale and did not fit to the above mentioned equation. Having such an equation allows us also to estimate the activity lost during the cuts and consequently better assess the tritium content of the whole cylinder.

Table 1 compares the tritium activity found in the first mm of the plasma exposed surface of the tile (first disk) and the bulk of the tile. The high percentage (72%) of tritium found in the bulk of cylinder 4 arises more from the low tritium concentration present in the surface of the sample located in a shadowed part of the tile rather than from the amount of tritium trapped in the bulk of the tile.

It is also remarkable that for cylinder 4 a strong diffusion seems to take place from the back side of the tile. Such a phenomenon was already observed for other tiles [19] but is not yet elucidated.

Table. 1. Tritium fraction in the bulk of various cylinders [#] retrieved from JET divertor tiles after the DTE1 campaign

Tile	Cyl. N°	Depth examined mm	Tritium in the 1 st mm mCi	Total tritium bulk+surf mCi	Bulk fraction %
3	1	37.2	1.08	1.82	41
3	2	31.2	0.79	1.24	36
3	4	32.4	0.33	1.19	72
4	1	35.3	2.68	6.98	62

[#] diam.7.8mm

3.2. AMS depth profiles

The AMS tritium profiles are very different from the profiles obtained by full combustion. The depth resolution is of the order of $0.3 \mu\text{m}$ instead of 1 mm.

An advantage of AMS is its ability to analyse different elements for the same sample giving a better picture of the sample composition. Since the carbon tiles in JET are coated beryllium, the profile of such an element is very useful to decide between an erosion or co-deposition area. The simultaneous depth profiling of D, T, and Be is illustrated in figure 5 for a JET graphite tile from the PTE campaign.

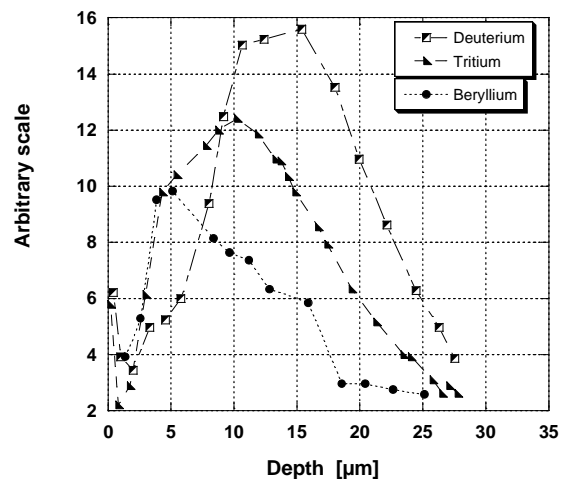


Fig.5. Beryllium, deuterium and tritium depth profiles measured by AMS for a JET CFC tile.

Figure 6 shows the deuterium and tritium AMS depth profiles for samples retrieved from tile 3 from the inner JET divertor. As illustrated the profiles of both elements are characterised by the presence of two zones. In the first zone corresponding to the co-deposited layer with a thickness of about $5 \mu\text{m}$ the relative concentration of both elements decreases sharply with the depth to reach an almost constant value representing the concentration of the second zone. In fact analyses for samples located deeper in the bulk showed a slight further decrease of that concentration which corresponds to the diffusion curve seen in the mm scale of the samples in figure 4.

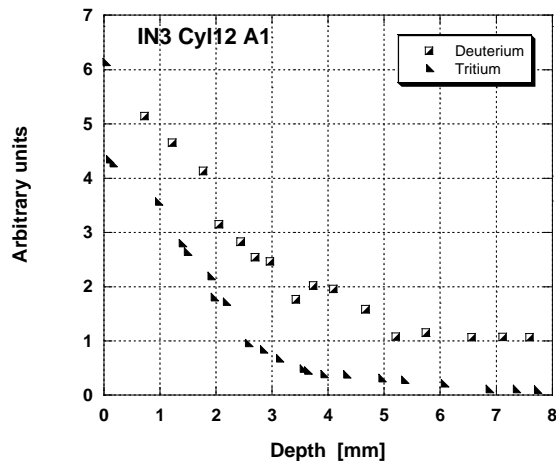


Fig. 6. AMS deuterium and tritium profiles for a plasma exposed disc from tile IN3_{s1} cylinder 12.

Tritium depth profiles measured by AMS for other carbon samples retrieved from JET or other fusion machines have already been reported by Friedrich et al. [21, 22].

4. Conclusions

Tritium retention in JET clearly occurs in the strike points region of the inner and outer divertor.

For CFC tiles a large fraction of the tritium is found in the bulk of the tile (up to 60% for tile 4) firmly fixed in the traps of the carbon net. The most probable mechanism involves tritium diffusion between the CFC cloths. This strongly depends on the tile temperature, tile location in JET and orientation of the cloths with respect to the scrape off layer.

The coring technique followed by a full combustion and liquid scintillation counting appears to be the most appropriate method for the absolute tritium determination on small discs.

In this respect deuterium and tritium measurements indicate that the inner divertor collects substantially higher amounts of tritiated species than the outer divertor, and clearly acts as a trap for large amounts of co-deposited material. The latter covers the inner and cooler part of

the divertor in zones not accessible by the plasma.

The inner divertor tiles show a clear diffusion profile. This mechanism immobilises in the bulk of the corresponding tiles (3, 4 and 7) substantial amounts of tritium (~ 40% for tile 3).

AMS analyses on the corresponding tiles have confirmed that the diffusion process is taking place for the deuterium as well.

The existence of large fractions of tritium in the bulk of these tiles represents an inventory that may affect the use of in-situ techniques for tritium detritiation. Simple isotopic exchange which treats only the surface would leave substantial amounts of tritium remaining in the bulk.

References.

- [1] G. Federici, Ch. Skinner et al., Nuclear Fusion 41 (2001) 1967.
- [2] H.W. Herrmann, S.J. Zweben, D.S. Darrow, J.R. Timberlake, G.P. Chong, A.A. Haasz, C.S. Pitcher, R.G. Mac Caulay-Newcombe, Nuclear Fusion 37 (1997) 293.
- [3] R.A. Causey, K.L. Wilson, J. Nucl. Mater. 138 (1986) 57.
- [4] M.E. Malinovski, R.A. Causey, J. Vac. Sci. Technol. A 6(3) (1988) 2130.
- [5] R.A. Langley, R.S. Blewer, J. Roth. J. Nucl. Mater. 76-77 (1978) 313.
- [6] A.T. Peacock, P.A. Andrew, D. Brennan, J.P. Coad, H. Hemmerich, S. Knipe, R.-D. Penzhorn, M. Pick, Fus. Eng. Design 49 (2000) 745.
- [7] A. v. Keudell, W. Jacob, J. Appl. Phys. 79 (1996) 1092.
- [8] D.E. Vance, M.E. Smith, G.R. Waterbury, LA-7716 UC, April 1979.
- [9] G. Sun, M. Friedrich, R. Grötzschel, W. Bürger, R. Berisch, C. Garcia-Rosales, J. Nucl. Mater. 246 (1997) 9.
- [10] M. Friedrich, W. Pilz, G. Sun, R.-D. Penzhorn, N. Bekris, R. Behrisch. C. Garcia-Rosales, Physica Scripta T94, 98-101, 2001.

-
- [11] J.W. Mellor, Inorganic and theoretical chemistry, Longmans, Green and Co, Vol. V, (1955) p 811.
- [12] M. Glugla, R. Lässer, T.L. Le, R.-D. Penzhorn, K.H. Simon, Fus. Eng. Design 49-50, (2000) 811.
- [13] Y. Iwai, T. Hayashi, K. Kobayashi, M. Nishi, Fus. Eng. Design 54, (2001) 523.
- [14] Gmelins Handbuch der Chemie, Kohlenstoff, Teil B, System Nr. 14, Verlag Chemie GmbH, Weinheim Bergstrasse, (1968), p. 796.
- [15] J.P. Coad, J. Nucl. Mater. 226 (1995) 156.
- [16] J.P. Coad, N. Bekris, J.D. Elder, S.K. Erents, D.E. Hole, G.F. Matthews, R.-D. Penzhorn, P.C. Stangeby, J. Nucl. Mater. 290-93 (2001) 224.
- [17] C.H. Skinner, C.A. Gentile, K.M. Young, J.P. Coad, J.T. Hogan, R.-D. Penzhorn, N. Bekris, 8th EPS Conference on Controlled Fusion and Plasma Physics, Madeira, Portugal, 18-22nd June, 2001.
- [18] R.-D. Penzhorn, J.P. Coad, N. Bekris; L. Doerr, M. Friedrich, W. Pilz, Fus. Eng. Design 56-57 (2001) 105.
- [19] J.P. Coad, M Rubel and C H Wu, J. Nucl. Mater. 241-243 (1997) 408.
- [20] R.-D. Penzhorn, N. Bekris; U. Berndt, J.P.Coad, H. Ziegler, W. Nägele, J. Nucl. Mater. 288 (2001) 170.
- [21] M. Friedrich, W. Pilz, G. Sun, R. Behrisch, C. Garcia-Rosales, N. Bekris, R.-D. Penzhorn, Nucl. Instrum. Methods B 161-163 (2000) 216-220.
- [22] M. Friedrich, W. Pilz, G. Sun, R. Behrisch, C. Garcia-Rosales, N. Bekris R.-D. Penzhorn, Nucl. Instrum. Methods B 172, 2000, 655-658.